In Vivo Adaptation of Hepatitis C Virus in Chimpanzees for Efficient Virus Production and Evasion of Apoptosis

Mohsan Saeed,[1,2] Masaaki Shiina,[3] Tomoko Date,[1] Daisuke Akazawa,[1] Noriyuki Watanabe,[1] Asako Murayama,[1] Tetsuro Suzuki,[1] Haruo Watanabe,[2,4] Nobuhiko Hiraga,[5] Michio Imamura,[5] Kazuaki Chayama,[5] Youkyung Choi,[6] Krzysztof Krawczynski,[6] T. Jake Liang,[7] Takaji Wakita,[1] and Takanobu Kato[1]

Hepatitis C virus (HCV) employs various strategies to establish persistent infection that can cause chronic liver disease. Our previous study showed that both the original patient serum from which the HCV JFH-1 strain was isolated and the cell culture–generated JFH-1 virus (JFH-1cc) established infection in chimpanzees, and that infected JFH-1 strains accumulated mutations after passage through chimpanzees. The aim of this study was to compare the *in vitro* characteristics of JFH-1 strains emerged in each chimpanzee at early and late stages of infection, as it could provide an insight into the phenomenon of viral persistence. We generated full-genome JFH-1 constructs with the mutations detected in patient serum-infected (JFH-1/S1 and S2) and JFH-1cc–infected (JFH-1/C) chimpanzees, and assessed their effect on replication, infectious virus production, and regulation of apoptosis in cell culture. The extracellular HCV core antigen secreted from JFH-1/S1-, S2-, and C-transfected HuH-7 cells was 2.5, 8.9, and 2.1 times higher than that from JFH-1 wild-type (JFH-1/wt) transfected cells, respectively. Single cycle virus production assay with a CD81-negative cell line revealed that the strain JFH-1/S2, isolated from the patient serum-infected chimpanzee at a later time point of infection, showed lower replication and higher capacity to assemble infectious virus particles. This strain also showed productive infection in human hepatocyte–transplanted mice. Furthermore, the cells harboring this strain displayed lower susceptibility to the apoptosis induced by tumor necrosis factor α or Fas ligand compared with the cells replicating JFH-1/wt. *Conclusion:* The ability of lower replication, higher virus production, and less susceptibility to cytokine-induced apoptosis may be important for prolonged infection *in vivo*. Such control of viral functions by specific mutations may be a key strategy for establishing persistent infection. (HEPATOLOGY 2011;00:000–000)

Currently, approximately 200 million people are infected with hepatitis C virus (HCV) and are at continuous risk of developing chronic liver diseases such as chronic hepatitis, liver cirrhosis, and hepatocellular carcinoma.[1,2] Although acute HCV infection elicits innate and adaptive immune responses, the virus successfully evades clearance in approximately 75% of infected individuals.[3,4] The mechanisms by

Abbreviations: Ag, antigen; CTL, cytotoxic T lymphocytes; FasL, Fas ligand; HCV, hepatitis C virus; JFH-1cc, cell culture–generated JFH-1 virus; JFH-1/wt, JFH-1 wild-type; MFI, mean fluorescence intensity; NK, natural killer; NS, nonstructural; PARP, poly(adenosine diphosphate ribose) polymerase; TNF-α, tumor necrosis factor α; TUNEL, terminal deoxynucleotidyl transferase–mediated deoxyuridine triphosphate nick-end labeling.

From the [1]Department of Virology II, National Institute of Infectious Diseases, Tokyo, Japan; the [2]Department of Infection and Pathology, Graduate School of Medicine, The University of Tokyo, Tokyo, Japan; the [3]Division of Gastroenterology, Tohoku University Graduate School of Medicine, Sendai, Japan; the [4]National Institute of Infectious Diseases, Tokyo, Japan; the [5]Department of Medicine and Molecular Science, Division of Frontier Medical Science, Programs for Biomedical Research, Graduate School of Biomedical Sciences, Hiroshima University, Hiroshima, Japan; the [6]Division of Viral Hepatitis, Center for Disease Control and Prevention, Atlanta, GA; and the [7]Liver Diseases Branch, National Institute of Diabetes and Digestive and Kidney Diseases, National Institutes of Health, Bethesda, MD.

Received November 26, 2010; accepted April 18, 2011.

Supported by grants-in-aid from the Japan Society for the Promotion of Science, the Ministry of Health, Labor, and Welfare of Japan, and the Ministry of Education, Culture, Sports, Science, and Technology, by the Research on Health Sciences Focusing on Drug Innovation from the Japan Health Sciences Foundation, and in part by the Intramural Research Program of the NIDDK, NIH (T. J. L.).

Tetsuro Suzuki is currently affiliated with the Department of Infectious Diseases, Hamamatsu University School of Medicine, Hamamatsu, Japan.

Address reprint requests to: Takanobu Kato, M.D., Ph.D., Department of Virology II, National Institute of Infectious Diseases, Tokyo, 162-8640, Japan. E-mail: takato@nih.go.jp; fax: (81)-3-5285-1161.

View this article online at wileyonlinelibrary.com.

DOI 10.1002/hep.24399

Potential conflict of interest: Nothing to report.

Additional Supporting Information may be found in the online version of this article.

which HCV leads to persistent infection at a high frequency are not yet fully understood. Lack of appropriate animal models, except chimpanzees, has rendered such studies difficult. Human hepatocyte-transplanted mice,[5,6] a useful small animal model to study HCV infection, are unsuitable to study the mechanisms of virus persistence because of a lack of B and T cell–mediated immunity.

HCV is a noncytopathic positive-stranded RNA virus of the *Flaviviridae* family. It primarily infects hepatocytes of humans and chimpanzees, where, thanks to error-prone RNA-dependent RNA polymerase, the infected virus accumulates a high number of mutations rapidly, thus providing opportunity for selection of viruses that have the ability to escape the immune system and establish persistent infection. Deciphering the strategies employed by HCV to establish persistence can be helpful in the development of new strategies to eradicate the virus and to stop disease progression. Until recently, the lack of an HCV strain having the ability to establish infection *in vivo* and *in vitro* was a substantial hindrance in studying the molecular mechanisms of virus persistence. This problem was solved by the identification of an HCV strain, JFH-1, that was isolated from a fulminant hepatitis patient and found to be capable of replicating and assembling infectious virus particles in chimpanzees as well as in cell culture.[7-10] This clone can be used to study the molecular mechanisms by which HCV evades the host immune system and causes chronic infection.

In a previous report, we inoculated patient serum from which the JFH-1 strain was originally isolated and cell culture–generated JFH-1 virus (JFH-1cc) into two different chimpanzees.[11] HCV established infection in both animals within 3 days of inoculation. In the JFH-1cc–infected chimpanzee, genome sequence of predominant infecting virus at week 2 was identical to JFH-1 wild-type (JFH-1/wt [in this study, this abbreviation was used instead of JFH-1 to distinguish it from other variant strains]), and the infecting virus has four synonymous and seven nonsynonymous mutations at week 7. In the JFH-1 patient serum–infected chimpanzee, 19 synonymous and six nonsynonymous mutations were observed in predominantly circulating virus at week 2, and this number increased to 35 synonymous and 17 nonsynonymous mutations at the later stage of infection course (week 23).[11] From these observations, we presumed that the isolates evolved in each chimpanzee at later stages of infection might have some advantage over the viruses isolated at earlier time points for survival in infected animals. Thus, in this study, we generated JFH-1 variants containing the mutations observed in these animals and assessed their effect on replication and infectious virus production in cell culture. Furthermore, we examined the effects of infection of these strains to tumor necrosis factor α (TNF-α)– or Fas ligand (FasL)–mediated apoptosis.

Materials and Methods

The complete Materials and Methods are provided in the Supporting Information.

Results

Effects of Mutations Identified in Chimpanzees. To investigate the effect of mutations on virus phenotype, we generated constructs containing the mutations observed in JFH-1 patient serum–infected chimpanzee and JFH-1cc–infected chimpanzee at various time points. The JFH-1 variants JFH-1/S1 and JFH-1/S2 contain the mutations observed in the patient serum–infected chimpanzee at week 2 and week 23, respectively, and JFH-1/C contains the mutations observed in the JFH-1cc–infected chimpanzee at week 7 (Supporting Table 1). The replication and virus production capacity of these variants in HuH-7 cells was compared with that of JFH-1/wt. After electroporation of *in vitro*–synthesized full-genome RNA of JFH-1/wt and variant strains, extracellular and intracellular HCV RNA and core antigen (Ag) were measured (Fig. 1). At day 5 posttransfection, all constructs displayed similar intracellular HCV RNA levels. However, extracellular HCV RNA level of JFH-1/C was 1.6 times higher than that of JFH-1/wt. Likewise, extracellular HCV RNA level of JFH-1/S2 was 3.4 times higher than that of JFH-1/S1 (Fig. 1A). Intracellular HCV core Ag levels of JFH-1/S2 and C were 240.9 $\pm$ 58.2 and 189.8 $\pm$ 42.1 fmol/mg protein, respectively, and were significantly lower ($P < 0.005$) than that of JFH-1/S1 (526.1 $\pm$ 58.2 fmol/mg protein) and JFH-1/wt (511.7 $\pm$ 32.9 fmol/mg protein) at day 1, but reached comparable levels at day 5 posttransfection. On the other hand, extracellular HCV core Ag level of JFH-1/C was 2.2 times higher than that of JFH-1/wt, and that of JFH-1/S2 was 3.6 times higher than that of JFH-1/S1 at day 5 posttransfection (Fig. 1B). Transfection efficiency of these strains, indicated by intracellular HCV core Ag levels at 4 hours posttransfection, was almost identical (data not shown).

Single Cycle Virus Production Assay. For detailed analysis of the effects of these mutations on different stages of the virus lifecycle, we used a Huh7-25 cell

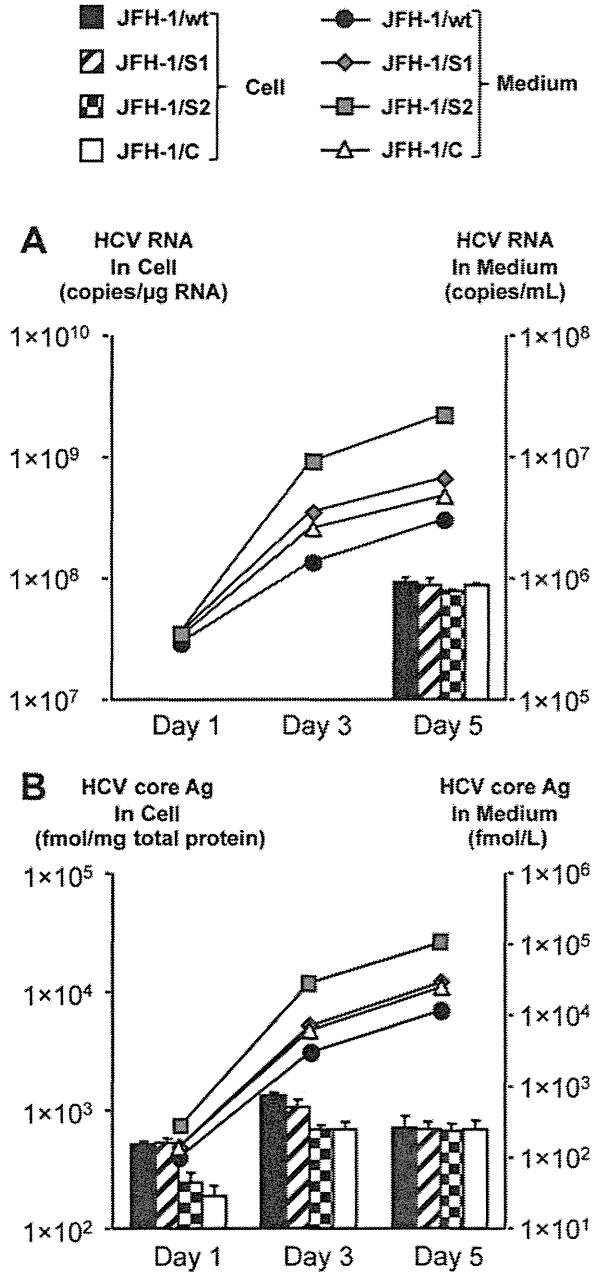

Fig. 1. Effects of *in vivo* adaptive mutations on virus production in HuH-7 cells. One million cells were transfected with 10 μg *in vitro*-transcribed RNA of JFH-1/wt, JFH-1/S1, JFH-1/S2, and JFH-1/C. (A) HCV RNA and (B) core Ag levels in cell lysates and medium were measured at the indicated time points. Assays were performed in triplicate, and data are presented as the mean ± SD.

line that lacks the surface expression of CD81, one of the cellular receptors for HCV entry. Three days after transfection with full-genome RNA of JFH-1/wt, JFH-1/S1, JFH-1/S2, and JFH-1/C, HCV RNA levels and infectivity titer were measured, and the specific infectivity was calculated (Table 1). Intracellular HCV RNA levels of JFH-1/C and JFH-1/S2 were lower than those of JFH-1/wt and S1, suggesting lower replication efficiency of these strains. However, the intracellular infectivity titers of JFH-1/C and JFH-1/S2 were 2.03 and 11.0 times higher than those of JFH-1/wt and JFH-1/S1, respectively ($P < 0.005$). Intracellular-specific infectivities (infectivity titer/HCV RNA copy number) of JFH-1/C and JFH-1/S2 showed more pronounced difference from those of JFH-1/wt and JFH-1/S1 (3.92 times and 12.9 times higher, respectively; $P < 0.005$). The infectious virus secretion rate (extracellular infectivity titer/intracellular infectivity titer) was not significantly different between JFH-1/wt and variant strains. These data indicate that mutations identified in chimpanzees at the later time point of infection led to reduced viral replication and increased assembly of infectious virus particles without any effect on viral release in cell culture.

Subgenomic Replicon Assay. To further confirm the replication efficiencies of strains observed in chimpanzees, we generated subgenomic replicons of JFH-1/wt, JFH-1/S1, JFH-1/S2, and JFH-1/C carrying the firefly luciferase reporter gene (SGR-JFH-1/Luc/wt, SGR-JFH-1/Luc/S1, SGR-JFH-1/Luc/S2, and SGR-JFH-1/Luc/C). *In vitro*–transcribed RNAs of these constructs were transfected into HuH-7 cells, and luciferase activity was measured to assess their replication capacity. The luciferase activities of SGR-JFH-1/Luc/C and SGR-JFH-1/Luc/S2 replicons were 7.30 and 7.33 times lower than those of SGR-JFH-1/Luc/wt and SGR-JFH-1/Luc/S1, respectively, at day 1 ($P < 0.00005$), suggesting attenuated replication capacities of variant replicons isolated from each animal at later time points of infection (Supporting Fig. 1A). The luciferase activity 4 hours after transfection was comparable, indicating similar levels of transfection efficiency (data not shown). Based on these data, we found that the mutations that emerged in nonstructural (NS)3-NS5B of JFH-1/S2 and JFH-1/C reduced the replication efficiency in cell culture.

Genomic Regions Responsible for Lower Replication and Higher Assembly of JFH-1/S2. To further clarify the genomic region responsible for lower replication efficiency and higher assembly rate of JFH-1/S2, we generated the chimeric constructs JFH-1/S2-wt and JFH-1/wt-S2 as described in the Supporting Materials and Methods. *In vitro*–transcribed RNAs of JFH-1/wt, JFH-1/S2, JFH-1/S2-wt, and JFH-1/wt-S2 were introduced into HuH-7 cells by electroporation and intracellular and extracellular HCV RNA and core Ag were measured. At day 5 posttransfection, all constructs displayed comparable intracellular HCV RNA levels (Fig. 2). However, extracellular HCV RNA levels of JFH-1/S2 and JFH-1/S2-wt were significantly

Table 1. Infectious Virus Production and Release of JFH-1/wt and Variants in Huh7-25 Cells

Strain	Intracellular			Extracellular	Secretion Ratio (Extracellular/ Intracellular)
	HCV RNA (copies/μg RNA)	Infectivity Titer (ffu/well)	Specific Infectivity (ffu/copies)	Infectivity Titer (ffu/well)	
JFH-1/wt	$7.75 \times 10^8 \pm 1.04 \times 10^8$	$4.21 \times 10^2 \pm 4.32 \times 10^1$	$2.09 \times 10^{-7} \pm 7.06 \times 10^{-8}$	$1.94 \times 10^3 \pm 3.76 \times 10^1$	4.6 ± 1.3
JFH-1/S1	$7.04 \times 10^8 \pm 8.49 \times 10^7$	$4.72 \times 10^2 \pm 5.63 \times 10^1$	$2.91 \times 10^{-7} \pm 6.00 \times 10^{-8}$	$3.02 \times 10^3 \pm 2.77 \times 10^2$	5.4 ± 2.0
JFH-1/S2	$4.16 \times 10^{8**} \pm 7.47 \times 10^6$	$5.19 \times 10^{3**} \pm 8.24 \times 10^1$	$3.76 \times 10^{-6**} \pm 7.01 \times 10^{-7}$	$3.23 \times 10^{4**} \pm 3.52 \times 10^3$	6.2 ± 3.0
JFH-1/C	$3.15 \times 10^{8*} \pm 5.02 \times 10^7$	$8.59 \times 10^{2*} \pm 4.81 \times 10^1$	$8.19 \times 10^{-7*} \pm 5.68 \times 10^{-8}$	$3.68 \times 10^3 \pm 3.02 \times 10^3$	4.3 ± 1.4
JFH-1/S2-wt	$7.07 \times 10^8 \pm 8.43 \times 10^7$	$4.40 \times 10^{3*} \pm 9.5 \times 10^1$	$2.73 \times 10^{-6*} \pm 2.35 \times 10^{-7}$	$3.0 \times 10^{4*} \pm 1.1 \times 10^3$	6.7 ± 0.7
JFH-1/wt-S2	$4.21 \times 10^{8*} \pm 1.97 \times 10^7$	$2.7 \times 10^2 \pm 2.9 \times 10^1$	$2.02 \times 10^{-7} \pm 4.0 \times 10^{-8}$	$1.7 \times 10^3 \pm 1.3 \times 10^2$	4.5 ± 0.4

Abbreviation: ffu, focus-forming units.
*$P < 0.005$ versus JFH-1/wt.
**$P < 0.005$ versus JFH-1/S1.

higher ($P < 0.0005$) than that of JFH-1/wt. On the other hand, extracellular RNA level of JFH-1/wt-S2 chimeric construct was lower than that of JFH-1/S2 and JFH-1/S2-wt and similar to that of JFH-1/wt. Likewise, extracellular core Ag levels of JFH-1/S2 and JFH-1/S2-wt were also significantly higher than that of JFH-1/wt. Intracellular HCV core Ag levels of JFH-1/S2 and JFH-1/wt-S2 on day 1 posttransfection were 240.9 ± 58.2 and 134.3 ± 17.1 fmol/mg protein, respectively, and were significantly lower ($P < 0.005$) than that of JFH-1/wt (526.1 ± 58.2 fmol/mg protein), whereas intracellular HCV core Ag level of JFH-1/S2-wt was comparable to that of JFH-1/wt. Transfection efficiency of these strains, indicated by intracellular HCV core Ag levels at 4 hours posttransfection, was almost identical (data not shown).

To further elucidate, we transfected Huh7-25 cells with *in vitro*–transcribed RNA of JFH-1/wt, JFH-1/S2, JFH-1/S2-wt, and JFH-1/wt-S2 and measured HCV RNA, core Ag, and infectivity titer in the cells and culture medium. Intracellular HCV RNA levels of JFH-1/S2 and JFH-1/wt-S2 were similar and lower than those of JFH-1/wt and JFH-1/S2-wt, suggesting mutations in NS3-NS5B were responsible for lower replication efficiency of JFH-1/S2 (Table 1). Intracellular infectivity titer of JFH-1/S2 and JFH-1/S2-wt was 12.3 and 10.4 times higher, respectively, than that of JFH-1/wt ($P < 0.005$) on day 3 posttransfection. The intracellular specific infectivities of JFH-1/S2 and JFH-1/S2-wt were significantly higher than that of JFH-1/wt (18 times and 13.1 times higher, respectively; $P < 0.005$). On the other hand, intracellular specific infectivity of JFH-1/wt-S2 was comparable to that of JFH-1/wt. The infectious virus secretion rate was not significantly different among all the constructs (Table 1). These data indicate that mutations emerged in the core-NS2 region of JFH-1/S2 are responsible for the enhanced assembly of infectious virus particles compared with JFH-1/wt.

Mapping Study for JFH-1/S2 Strain. Because our experiments with JFH-1/S2 subgenomic replicon and JFH-1/wt-S2 chimeric construct showed that mutations emerged in the NS3-NS5B region are responsible for reduced replication efficiency of JFH-1/S2, we performed mapping studies by generating various JFH-1 subgenomic replicons, each containing the mutations observed in individual nonstructural protein. Although mutations in NS4B and NS5A were associated with attenuated replication capacity of JFH-1, the most significant decrease in replication was observed with NS5B mutations (Supporting Fig. 1B).

For detailed analysis of mutations responsible for higher assembly, *in vitro*–transcribed RNAs of JFH-1/wt, JFH-1/S2, JFH-1/S2-wt, JFH-1/N397S, JFH-1/L752V, JFH-1/S2-NS2 (containing mutations G838R, A878V, and V881A), JFH-1/G838R, and JFH-1/A878V were transfected into Huh7-25 cells, and intracellular-specific infectivities were compared (Supporting Table 2). As reported previously, JFH1/G838R showed higher intracellular specific infectivity than that of JFH-1/wt, but could not reach the level of JFH-1/S2 or JFH-1/S2-wt. Among the mutants, intracellular specific infectivities of JFH1/L752V, JFH1/NS2, and JFH1/G838R were 4.02, 5.42, and 3.07 times higher than that of JFH-1/wt, but those of JFH1/N397S and JFH1/A878V were similar to that of JFH-1/wt. Thus, the combination of mutations in P7 and NS2 was found to contribute to the higher assembly of the JFH-1/S2 strain.

Human Hepatocyte–Transplanted Mouse Assay. To assess the *in vivo* infectivity of these strains, we inoculated culture medium containing 10^7 copies (HCV RNA titer measured by RTD-PCR) of JFH-1/wt, JFH-1/S1, JFH-1/S2, and C viruses into human

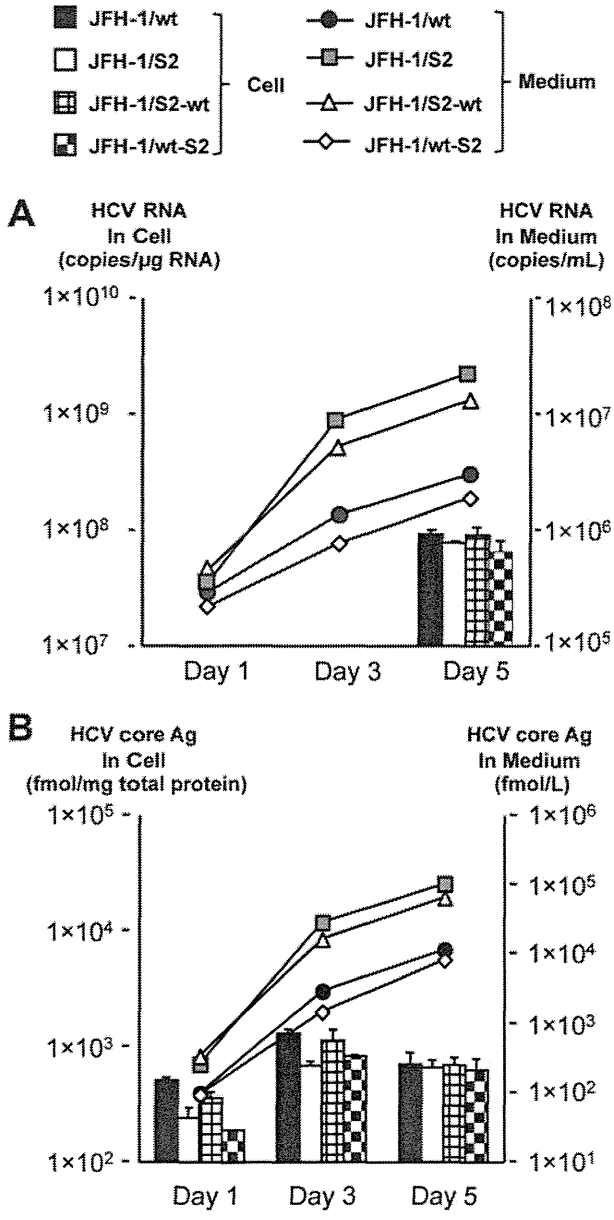

Fig. 2. Virus production of JFH-1/S2 chimeric constructs in HuH-7 cells. One million cells were transfected with 10 μg *in vitro*-transcribed RNA of JFH-1/wt, JFH-1/S2, JFH-1/S2-wt, and JFH-1/wt-S2. (A) HCV RNA and (B) core Ag levels in cell lysates and medium were measured at the indicated time points. Assays were performed in triplicate, and data are presented as the mean ± SD.

hepatocyte-transplanted mice. Two mice were used for each virus. Two weeks after intravascular inoculation, all mice but one became HCV RNA–positive (Fig. 3). Two mice died 3 weeks after inoculation; one was inoculated with JFH-1/wt and had developed infection, and the other was inoculated with JFH-1/C and died without developing infection. HCV RNA levels in infected mice fluctuated, ranging from 10^6 to 10^9 copies/mL. We could not observe much difference of infected HCV RNA titer among these inoculated mice. Sequence analyses of the complete open reading frames revealed that infecting JFH-1/wt virus and variant strains had no nonsynonymous mutations at the time of development of infection. From these data, we concluded that not only JFH-1/wt virus but also JFH-1/S1, JFH-1/S2, and JFH-1/C viruses were able to establish productive infection in human hepatocyte-transplanted mice.

Apoptosis Induction Assay. To investigate the survival strategy against the host defense system, we examined the susceptibility of JFH-1/wt and variant strains to TNF-α–mediated apoptosis induction. After transfection with *in vitro*–transcribed RNA of JFH-1/wt, JFH-1/S1, JFH-1/S2, and JFH-1/C, Huh-7.5.1 cells were exposed to TNF-α plus actinomycin D. Without exposure, apoptosis was observed in a limited number of HCV-positive cells (Supporting Fig. 2A). Forty-eight hours later, cells were harvested, fixed, and

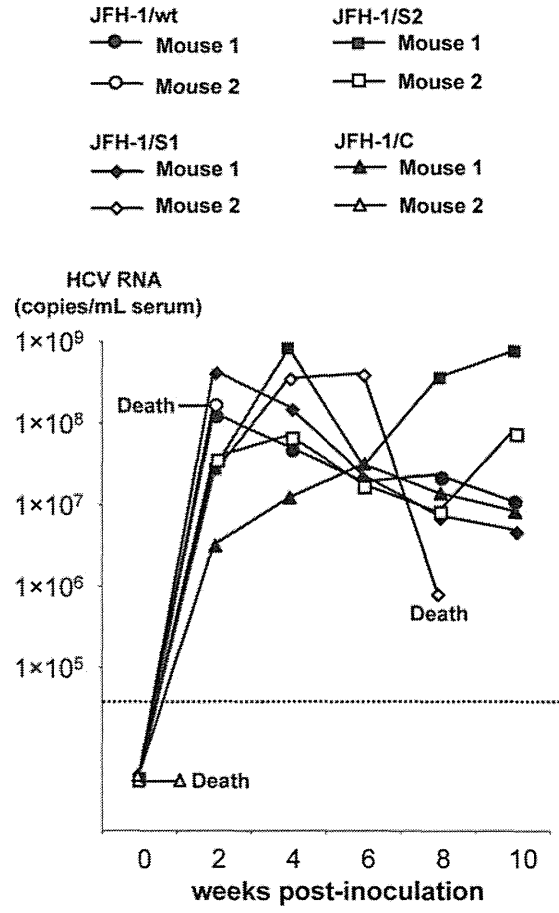

Fig. 3. *In vivo* infection study of JFH-1/wt and its variants in human hepatocyte-transplanted mice. Cell culture medium containing 1 × 10^7 HCV RNA copies of JFH-1/wt, JFH-1/S1, JFH-1/S2, and JFH-1/C were inoculated into human hepatocyte-transplanted mice, and HCV RNA levels in mice serum were monitored.

subjected to terminal deoxynucleotidyl transferase–mediated deoxyuridine triphosphate nick-end labeling (TUNEL) assay and anti-HCV NS5A staining. The effects of JFH-1/wt, JFH-1/S1, JFH-1/S2, and JFH-1/C transfection on apoptosis induction were determined by calculating the ratio of apoptosis between HCV-positive and HCV-negative populations and expressed as an apoptosis induction index. After treatment of JFH-1/wt–transfected cells with TNF-α, apoptosis was observed in 36.8% of the HCV-positive population and in 19.3% of the HCV-negative population, and the apoptosis induction index was 1.85 ± 0.06 (Fig. 4). The apoptosis induction indexes of JFH-1/S1–transfected and JFH-1/C– transfected cells were 1.23 ± 0.06 and 1.16 ± 0.10, respectively, suggesting lower susceptibility to apoptosis induction compared with JFH-1/wt. On the other hand, the apoptosis induction index of JFH-1/S2 was 0.74 ± 0.17, which was substantially lower than that of JFH-1/wt, demonstrating the more reduced apoptosis in the cells harboring this strain. Similar results were obtained by treatment with FasL plus actinomycin D (Supporting Fig. 2B). To confirm the lower susceptibility of JFH-1/S2–transfected cells, apoptosis was also detected by staining with anticleaved poly(adenosine diphosphate ribose) polymerase (PARP) antibody. The apoptosis induction indexes of JFH-1/wt and JFH-1/S2–transfected cells were 2.28 ± 0.24 and 1.15 ± 0.14, respectively, and were consistent with TUNEL assay (Fig. 5). Although the HCV NS5A-positive rate in JFH-1/S2–transfected cells was higher than that in JFH-1/wt, the mean fluorescence intensity of the NS5A-positive population in JFH-1/S2–transfected cells was significantly lower (185.0 ± 8.7) than that in JFH-1/wt–transfected cells (395.0 ± 98.0), corresponding to the observed phenotype of the JFH-1/S2 strain in the single cycle virus production assay (i.e., lower replication efficiency and rapid spread to surrounding cells).

To clarify the genomic region responsible for lower susceptibility of JFH-1/S2 to cytokine-induced apoptosis, we examined the effect of TNF-α on the cells carrying subgenomic reporter replicons. The apoptosis induction index of SGR-JFH1/Luc/S2–transfected cells was lower than that of SGR-JFH1/Luc/wt–transfected cells (Supporting Fig. 2C); however, the difference was not as pronounced as with full-genome constructs, indicating that mutations in the NS3-NS5B region contribute to lower susceptibility of JFH-1/S2 to cytokine-induced apoptosis, but they are not sufficient to explain the difference between JFH-1/wt and JFH-1/S2. We confirmed these results by use of the chimeric

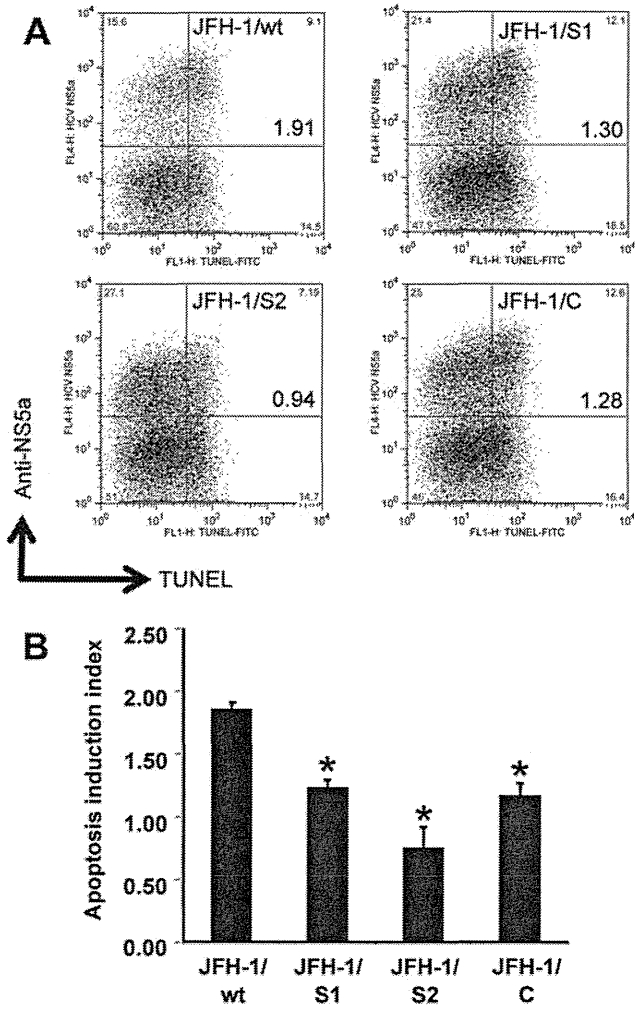

Fig. 4. Apoptosis induction in Huh-7.5.1 cells transfected with JFH-1/wt and its variants. (A) Three million cells were transfected with 3 μg *in vitro*-transcribed full-genome RNA of JFH-1/wt, JFH-1/S1, JFH-1/S2, and JFH-1/C. Forty-eight hours later, apoptosis was induced by exposing cells to 20 ng/mL TNF-α plus 50 ng/mL actinomycin D. Cells were harvested after 48 hours of treatment and subjected to TUNEL and anti-HCV NS5A staining. Dot plots show HCV replication and apoptosis at the single cell level. Quadrant gates were determined using unstained and a terminal deoxynucleotidyltrasferase-untreated control in each culture condition. The clone names and apoptosis induction indexes are indicated in the upper right box. (B) Apoptosis induction indexes of JFH-1/wt–, JFH-1/S1–, JFH-1/S2–, and JFH-1/C– transfected cells. The mean ± SD of three independent experiments is shown. $^*P < 0.005$ versus JFH-1/wt.

constructs JFH-1/S2-wt and JFH-1/wt-S2. The apoptosis induction indexes of JFH-1/S2-wt–transfected and JFH-1/wt-S2–transfected cells were 1.42 ± 0.13 and 1.71 ± 0.08, respectively (Fig. 5). These data indicate that both structural and nonstructural regions of JFH-1/S2 were associated with lower susceptibility to cytokine-induced apoptosis, although mutations in core-NS2 seemed to have higher contribution toward this phenotype. Together, these results indicate that the JFH-1/S2 strain, which was selected after passage in

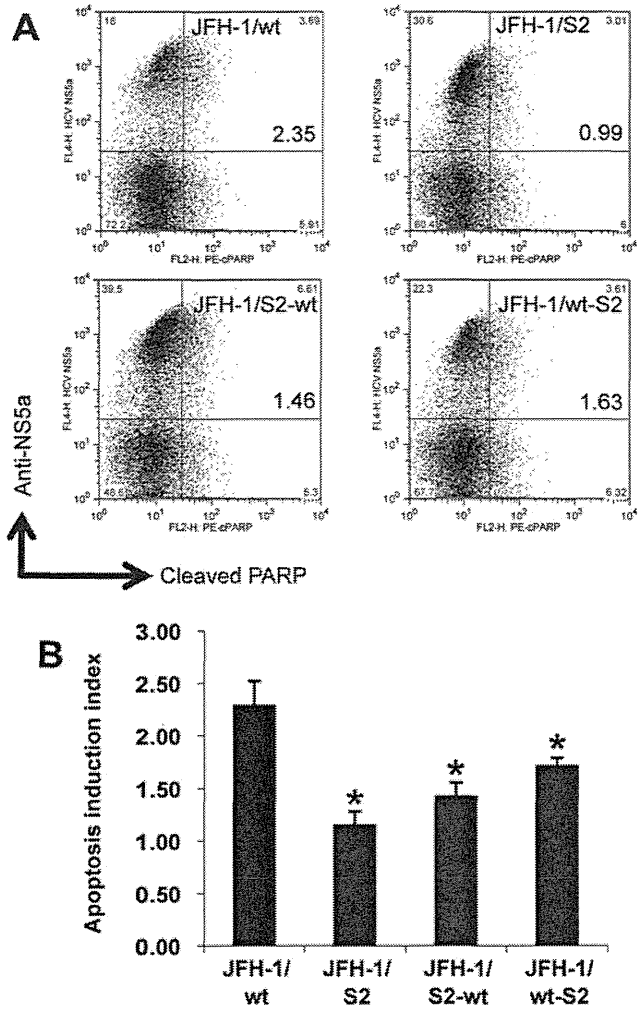

Fig. 5. Apoptosis induction in Huh-7.5.1 cells transfected with JFH-1/wt, JFH-1/S2, and their chimeric constructs. (A) Three million cells were transfected with 3 μg *in vitro*-transcribed full-genome RNA of JFH-1/wt, JFH-1/S2, JFH-1/S2-wt, and JFH-1/wt-S2. Apoptosis was induced by exposing cells to 20 ng/mL TNF-α plus 50 ng/mL actinomycin D and detected by anticleaved PARP staining. The clone names and apoptosis induction indexes are indicated in the upper right box. (B) Apoptosis induction indexes of JFH-1/wt-, JFH-1/S2-, JFH-1/S2-wt-, and JFH-1/wt-S2-transfected cells. The mean ± SD of three independent experiments is shown. *$P < 0.05$ versus JFH-1/wt.

the patient serum–infected chimpanzee, acquired less susceptibility to the cytokine-induced apoptosis.

Discussion

HCV develops chronic infection in the vast majority of infected patients[1]; however, the mechanisms of its persistence are still under investigation. Many viruses have evolved different strategies to cope with host immune systems, thus causing the development of persistent infection. For example, some viruses interfere with the major histocompatibility complex class I presentation of viral antigens, whereas others modulate lymphocyte and macrophage functions, including cytokine production.[12-16] In our previous study, we detected an increasing number of mutations in the HCV genome isolated from JFH-1 patient serum–infected chimpanzees. Thus, we reasoned that these detected mutations might have imparted some advantage to this virus for long-time survival. To examine this hypothesis, we compared the phenotypes of JFH-1 variant strains emerged at early and late stages of infection in JFH-1 patient serum–infected and JFH-1cc–infected chimpanzees and found that the JFH-1/S2 strain isolated from the patient serum–infected chimpanzee at a later time point of infection replicated slowly, produced more infectious viruses, and displayed reduced susceptibility to cytokine-induced apoptosis.

The JFH-1 variant strain JFH-1/C, which contains seven nonsynonymous mutations identified in the JFH-1cc–infected chimpanzee at week 7, showed comparatively slower replication kinetics and slightly enhanced infectious virus production in cell culture. The intracellular specific infectivity of this strain in Huh7-25 cells was 3.9 times higher than that of JFH-1/wt (Table 1). These characteristics might have imparted some advantage to this strain for establishing productive infection in the chimpanzee. The other JFH-1 variant strains, JFH-1/S1 and JFH-1/S2, contain 6 and 17 nonsynonymous mutations identified in the JFH-1 patient serum–infected chimpanzee at weeks 2 and 23 postinfection, respectively. Replication kinetics and infectious virus production of the JFH-1/S1 strain were comparable to that of JFH-1/wt in cultured cells (Fig. 1, Table 1). In contrast, the JFH-1/S2 strain showed lower replication efficiency. Although the intracellular HCV RNA level of this strain in Huh7-25 cells was lower than that of JFH-1/wt and JFH-1/S1, and almost the same as that of JFH-1/C (Table 1), intracellular specific infectivity was 18.0 and 12.9 times higher than that of JFH-1/wt and JFH-1/S1, respectively, suggesting a significant increase in the assembly of infectious virus particles ($P < 0.005$, Table 1). The enhanced capacity of this strain to assemble infectious virus particles resulted in a higher extracellular infectivity titer that contributed to the rapid spread of virus to surrounding cells. Flow cytometry analyses of cells transfected with JFH-1/wt and variant strains revealed that the percentage of the HCV NS5A-positive population in JFH-1/S2–transfected cells was higher, but the mean fluorescence intensity of the anti-NS5A signal was lower than that in JFH-1/wt–transfected cells, thus confirming higher spread and lower replication of this strain. Taken together, both JFH-1/C and JFH-1/S2 exhibited a tendency toward

decreased replication and increased infectious virus production. However, the extent of enhanced virus production was substantially lower in JFH-1/C than in JFH-1/S2, which might have led to the earlier elimination of infection in the JFH-1cc–infected chimpanzee. In other words, the potency of infectious virus production and spread seems to correspond to the duration of infection in infected animals.

The association between a lower replication efficiency and persistent infection is still unclear. It has been reported that an escape mutant with an amino acid substitution at the cytotoxic T lymphocyte (CTL) epitope in the NS3 region exhibits lower NS3/4 protease activity and replication capacity *in vitro*.[17,18] The JFH-1/S2 strain contains the T1077A mutation in the NS3 region (Supporting Table 1), and this mutation is located close to mutations reported to be associated with immune evasion and lower replication.[17] Thus, the lower replication efficiency of the JFH-1/S2 strain may be a result of an immune escape mutation at the expense of viral fitness. Meanwhile, we cannot deny the advantage of lower replication in establishing persistent infection. Lower replication may contribute to the avoidance of major histocompatibility class I–mediated antigen presentation and to escape from the host immune system. Either way, by acquiring the ability to produce more viral particles, the JFH-1/S2 strain could rapidly spread to surrounding cells, irrespective of its lower replication efficiency. Importantly, these emerged mutations did not attenuate *in vivo* infectivity, unlike cell culture adaptive mutations reported to cause attenuated infection *in vivo*.[19] Upon inoculation into human hepatocyte–transplanted mice, JFH-1/S1, JFH-1/S2, and JFH-1/C strains could establish infection without any mutations, produced levels of viremia similar to JFH-1/wt, and persisted for a similar observed period of infection (Fig. 2). This observation is different from that in chimpanzees, where JFH-1/wt and JFH-1/C strains were eliminated earlier than JFH-1/S2. In contrast to chimpanzees, human hepatocyte–transplanted mice lack a CTL and natural killer (NK) cell–mediated immune system, which could be responsible for this difference.[6] Taken together, our results suggest that along with efficient infectious virus production, the JFH-1/S2 strain might have acquired an advantage that helps it evade the CTL and NK cell–mediated immune system.

Apoptosis of virus-infected cells by the immune system is crucial as a general mechanism of clearing infections.[20,21] The J6/JFH-1 chimeric virus has been reported to exhibit proapoptotic characteristics in cell culture.[22] However, because HCV needs to escape the host immune system in order to establish chronic infection, immune cell–mediated apoptosis may be inhibited in infected hepatocytes. In the liver, HCV-infected hepatocytes are eliminated by targeted apoptosis induced by NK cells, macrophages, and CTLs with ligand-mediated and receptor-mediated signals such as TNF-α, FasL, and TNF-related apoptosis–inducing ligand.[23-26] Thus, we used TNF-α to mimic natural immunomediated apoptosis and found that the JFH-1/S2–replicating cells have lower susceptibility to the apoptosis induced by these cytokines. In JFH-1/S2–transfected cells, TNF-α–induced apoptosis detected by TUNEL assay was substantially lower than that of JFH-1/wt–transfected cells (Fig. 4). We confirmed it by staining with anticleaved PARP. In complete agreement with the results produced by way of TUNEL assay, the number of anticleaved PARP stained cells among JFH-1/S2–infected cells was significantly lower than that among JFH-1/wt–infected cells (Fig. 5). In our previous study, we reported that HCV-specific immune responses with T cell proliferation and interferon-γ production were maintained until the disappearance of viremia in the patient serum–infected chimpanzee.[11] This finding indicates that continuous selection pressure in the infected chimpanzee might have contributed to the emergence of a clone with an ability to escape the cytokine-induced apoptosis. We are not sure whether this phenotype of JFH-1/S2 is due to its lower replication efficiency and thus lower production of HCV proteins. The accumulation of viral proteins might predispose cells to the apoptosis induced by TNF-α. To answer this question, it will be necessary to investigate the genomic regions of JFH-1/S2 and cellular host factors responsible for the ability of this strain to escape the apoptosis.

By way of mapping analysis for JFH-1/S2, we could determine responsible regions; NS5B was for lower replication efficiency (Supporting Fig. 1B), and P7 and NS2 were for enhanced viral particle assembly (Supporting Table 2). For the evasion of apoptosis, we could not specify the responsible region, because both chimeric constructs, JFH-1/S2-wt and JFH-1/wt-S2, showed less susceptibility to cytokine-induced apoptosis to a certain extent. These data indicate that both structural and nonstructural regions might have contributed to the acquisition of this phenotype. Previously, a potent antiapoptotic effect of the HCV NS5A protein was described.[27] NS5A interacts with Bin1, which is a nucleocytoplasmic c-Myc–interacting protein with tumor suppressor and apoptotic properties, thus inhibiting Bin1-

associated apoptosis. Because JFH-1/S2 contains several mutations in the NS5A region (Supporting Table 1), one or more mutations in this protein may be associated with antiapoptotic effects.

In conclusion, we demonstrated that the JHF-1/S2 strain acquired phenotypes of lower replication, higher virus production, and less susceptibility to cytokine-induced apoptosis. These phenotypes were associated with mutations that emerged 23 weeks after infection in a chimpanzee, and might have contributed to long-term infection *in vivo*. Such control of viral functions by specific mutations may be a key viral strategy to establish persistent infection.

Acknowledgment: We are grateful to Francis V. Chisari for providing the Huh-7.5.1 cell line and Nao Sugiyama for technical assistance.

References

1. Liang TJ, Rehermann B, Seeff LB, Hoofnagle JH. Pathogenesis, natural history, treatment, and prevention of hepatitis C. Ann Intern Med 2000;132:296-305.
2. Feld JJ, Liang TJ. Hepatitis C—identifying patients with progressive liver injury. HEPATOLOGY 2006;43:S194-S206.
3. Thimme R, Oldach D, Chang KM, Steiger C, Ray SC, Chisari FV. Determinants of viral clearance and persistence during acute hepatitis C virus infection. J Exp Med 2001;194:1395-1406.
4. Thimme R, Bukh J, Spangenberg HC, Wieland S, Pemberton J, Steiger C, et al. Viral and immunological determinants of hepatitis C virus clearance, persistence, and disease. Proc Natl Acad Sci U S A 2002;99:15661-15668.
5. Mercer DF, Schiller DE, Elliott JF, Douglas DN, Hao C, Rinfret A, et al. Hepatitis C virus replication in mice with chimeric human livers. Nat Med 2001;7:927-933.
6. Tateno C, Yoshizane Y, Saito N, Kataoka M, Utoh R, Yamasaki C, et al. Near completely humanized liver in mice shows human-type metabolic responses to drugs. Am J Pathol 2004;165:901-912.
7. Kato T, Furusaka A, Miyamoto M, Date T, Yasui K, Hiramoto J, et al. Sequence analysis of hepatitis C virus isolated from a fulminant hepatitis patient. J Med Virol 2001;64:334-339.
8. Wakita T, Pietschmann T, Kato T, Date T, Miyamoto M, Zhao Z, et al. Production of infectious hepatitis C virus in tissue culture from a cloned viral genome. Nat Med 2005;11:791-796.
9. Zhong J, Gastaminza P, Cheng G, Kapadia S, Kato T, Burton DR, et al. Robust hepatitis C virus infection in vitro. Proc Natl Acad Sci U S A 2005;102:9294-9299.
10. Lindenbach BD, Evans MJ, Syder AJ, Wolk B, Tellinghuisen TL, Liu CC, et al. Complete replication of hepatitis C virus in cell culture. Science 2005;309:623-626.
11. Kato T, Choi Y, Elmowalid G, Sapp RK, Barth H, Furusaka A, et al. Hepatitis C virus JFH-1 strain infection in chimpanzees is associated with low pathogenicity and emergence of an adaptive mutation. HEPATOLOGY 2008;48:732-740.
12. Johannessen I, Crawford DH. In vivo models for Epstein-Barr virus (EBV)-associated B cell lymphoproliferative disease (BLPD). Rev Med Virol 1999;9:263-277.
13. Oglesbee MJ, Pratt M, Carsillo T. Role for heat shock proteins in the immune response to measles virus infection. Viral Immunol 2002;15:399-416.
14. Stevenson PG, Boname JM, de Lima B, Efstathiou S. A battle for survival: immune control and immune evasion in murine gamma-herpesvirus-68 infection. Microbes Infect 2002;4:1177-1182.
15. Alcami A. Viral mimicry of cytokines, chemokines and their receptors. Nat Rev Immunol 2003;3:36-50.
16. Wilkinson GW, Tomasec P, Stanton RJ, Armstrong M, Prod'homme V, Aicheler R, et al. Modulation of natural killer cells by human cytomegalovirus. J Clin Virol 2008;41:206-212.
17. Soderholm J, Ahlen G, Kaul A, Frelin L, Alheim M, Barnfield C, et al. Relation between viral fitness and immune escape within the hepatitis C virus protease. Gut 2006;55:266-274.
18. Uebelhoer L, Han JH, Callendret B, Mateu G, Shoukry NH, Hanson HL, et al. Stable cytotoxic T cell escape mutation in hepatitis C virus is linked to maintenance of viral fitness. PLoS Pathog 2008;4:e1000143.
19. Bukh J, Pietschmann T, Lohmann V, Krieger N, Faulk K, Engle RE, et al. Mutations that permit efficient replication of hepatitis C virus RNA in Huh-7 cells prevent productive replication in chimpanzees. Proc Natl Acad Sci U S A 2002;99:14416-14421.
20. Kagi D, Seiler P, Pavlovic J, Ledermann B, Burki K, Zinkernagel RM, et al. The roles of perforin- and Fas-dependent cytotoxicity in protection against cytopathic and noncytopathic viruses. Eur J Immunol 1995;25:3256-3262.
21. Kagi D, Vignaux F, Ledermann B, Burki K, Depraetere V, Nagata S, et al. Fas and perforin pathways as major mechanisms of T cell-mediated cytotoxicity. Science 1994;265:528-530.
22. Deng L, Adachi T, Kitayama K, Bungyoku Y, Kitazawa S, Ishido S, et al. Hepatitis C virus infection induces apoptosis through a Bax-triggered, mitochondrion-mediated, caspase 3-dependent pathway. J Virol 2008;82:10375-10385.
23. Kafrouni MI, Brown GR, Thiele DL. Virally infected hepatocytes are resistant to perforin-dependent CTL effector mechanisms. J Immunol 2001;167:1566-1574.
24. Guicciardi ME, Gores GJ. Apoptosis: a mechanism of acute and chronic liver injury. Gut 2005;54:1024-1033.
25. Fischer R, Baumert T, Blum HE. Hepatitis C virus infection and apoptosis. World J Gastroenterol 2007;13:4865-4872.
26. Stegmann KA, Bjorkstrom NK, Veber H, Ciesek S, Riese P, Wiegand J, et al. Interferon-alpha-induced TRAIL on natural killer cells is associated with control of hepatitis C virus infection. Gastroenterology 2010;138:1885-1897.
27. Nanda SK, Herion D, Liang TJ. The SH3 binding motif of HCV NS5A protein interacts with Bin1 and is important for apoptosis and infectivity. Gastroenterology 2006;130:794-809.

SUPPORTING INFORMATION

MATERIALS and METHODS

Cell Culture

HuH-7 and its derivative cell lines, Huh-7.5.1 provided by Francis Chisari (Scripps Research Institute, La Jolla, CA) and Huh7-25 were used in this study (1, 2). The HuH-7 derivative cell line Huh7-25, which lacks CD81 expression, was reported previously (2). Culture condition for these cell lines was described previously (3).

Plasmid Construction and RNA Transfection

The mutations identified in the JFH-1 patient serum inoculated chimpanzee at week 2 and week 23 were introduced into the pJFH-1 plasmid by use of amplified PCR fragments to determine the full-ORF sequence of infected viruses or by site-directed mutagenesis, and these plasmids were named pJFH-1/S1 and S2, respectively (Supporting Table 1). Likewise, the pJFH-1/C plasmid was generated with mutations identified in the JFH-1cc inoculated chimpanzee at week 7 (Supporting Table 1). Plasmids of pJFH-1/S2-wt and pJFH-1/wt-S2 were generated by replacing the core-NS2 and NS3-NS5B region of JFH-1/wt with the corresponding region of pJFH-1/S2, respectively. To assess the responsible region for higher assembly capacity, we introduced mutations observed in core-

NS2 region of pJFH1/S2 into pJFH1, and generated pJFH1/N397S containing mutation in E2, pJFH1/L752V containing mutation in P7, pJFH1/S2-NS2 containing mutations G838R, A878V and V881A in NS2, and pJFH1/A878V containing of mutations in NS2. The construct pJFH1/G838R containing one of mutations in NS2 was reported previously (3). Subgenomic replicon constructs containing the firefly luciferase reporter gene were synthesized by substituting the non-structural region of the pSGR-JFH1/Luc plasmid (4) with the corresponding regions of pJFH1/S1, S2 and C plasmids, and were named pSGR-JFH1/Luc/wt, S1, S2, and C, respectively. To identify the responsible region for lower replication efficiency of pJFH1/S2 strain, we also synthesized reporter subgenomic replicons containing mutations in NS3, NS4B, NS5A and NS5B of pJFH1/S2, and named pSGR-JFH1/Luc/S2-NS3, S2-NS4B, S2-NS5A and S2-NS5B, respectively. To prepare RNA for transfection, *in vitro* transcription was performed with linearized plasmids using a MEGAscript T7 kit (Ambion, Austin, TX) according to the manufacturer's recommendations. Electroporation was performed with cytomix as described (5,6).

Quantification of HCV RNA and Core Antigen

Total RNA was extracted with a QIAamp Viral RNA kit (QIAGEN, Valencia, CA) from 140 μL of culture medium or with an RNeasy mini kit (QIAGEN) from the harvested cell pellet. Real-time quantitative RT-PCR was performed to determine the copy numbers of HCV RNA as described previously

(7). The concentration of HCV core antigen (Ag) in filtered culture medium and cell lysates was determined by an HCV core Ag ELISA kit (Ortho Clinical Diagnostics, Tokyo, Japan) as described previously (8). The concentration of total RNA and total protein in the cells was determined using a Nanodrop Spectrophotometer ND-1000 (Thermo Scientific, Rockford, IL) and BSA™ Protein Assay kit (Thermo Scientific), respectively.

Titration of HCV Infectivity

Culture medium was serially diluted 5-fold in complete DMEM and used to infect naïve Huh-7.5.1 cells seeded 24 h earlier in poly-D-lysine coated flat-bottom 96-well plates (CORNING, Corning, NY) at a density of 1×10^4 cells per well. Three days after infection, HCV-positive cells were detected with mouse monoclonal antibody recognizing core protein (clone 2H9) and visualized with Alexa Fluor 488 anti-mouse secondary antibody (Invitrogen). The infectivity titer was expressed as focus-forming units per mL of supernatant (ffu/mL), expressing the mean number of HCV core-positive foci detected at the highest dilutions. The intracellular infectivity and specific intracellular infectivity titer were determined as described previously (3).

Infection Study with Human Hepatocyte-transplanted Mice

To generate human hepatocyte-transplanted mice, urokinase-type plasminogen activator (uPA)+/+ and severe combined immunodeficiency

(SCID)+/+ mice were transplanted with human hepatocytes as described previously (9). All mice were transplanted with frozen human hepatocytes obtained from the same donor. Infection, extraction of serum samples, and euthanasia were performed after anesthetizing mice with ether. The concentration of serum human albumin, which correlates with the repopulation index, was measured in mice as described previously (9). All animal protocols described in this study were performed in accordance with the guidelines of the local committee for animal experiments. The experimental protocol was approved by the Ethics Review Committee for Animal Experimentation of the Graduate School of Biomedical Sciences, Hiroshima University, Hiroshima, Japan. To determine the sequences of infected virus in these mice, viral RNA extracted from mouse serum was amplified by RT-PCR with primer sets for seven overlapping fragments covering the whole ORF and subjected to direct sequencing.

Apoptosis Induction Assay

To assess the induction of apoptosis, JFH-1/wt, S1, S2, and C transfected cells were treated with TNF-α (20 ng/mL) plus Actinomycin D (Act D; 50 ng/mL) or FasL (100 ng/mL) plus Act D (50 ng/mL). Cells, including floating cells, were collected 36 h later and detected for apoptosis by flow cytometry (10). The extent of apoptosis was determined either by terminal deoxynucleotidyltrasferase (TdT) mediated dUTP nick end-labeling (TUNEL)

assay (Apo-Direct kit; BD Biosciences, San Diego, CA) or by staining the cells with mouse anti-cleaved poly [ADP-Ribose] polymerase (PARP) antibody (BD Pharmingen, San Diego, CA). HCV positive cells were detected by staining with anti-HCV NS5a monoclonal antibody and Alexa-647 conjugated anti-mouse IgG secondary antibody. The ratio of apoptosis among HCV positive and negative populations was analyzed at the single cell level using a FACSCalibur flow cytometer (BD, Franklin Lakes, NJ) and CellQuest software (BD). The apoptosis induction index was calculated as follows: the ratio of apoptotic cells in the HCV-positive population divided by the ratio of apoptotic cells in the HCV-negative population.

Statistical analysis

Student's *t*-test was performed to evaluate the significance of results. $P < 0.05$ was considered significant.

References

1. Zhong J, Gastaminza P, Cheng G, Kapadia S, Kato T, Burton DR, Wieland SF, Uprichard SL, Wakita T, Chisari FV. Robust hepatitis C virus infection in vitro. Proc Natl Acad Sci U S A 2005;102:9294-9299.

2. Akazawa D, Date T, Morikawa K, Murayama A, Miyamoto M, Kaga M, Barth H, Baumert TF, Dubuisson J, Wakita T. CD81 expression is important for the permissiveness of Huh7 cell clones for heterogeneous hepatitis C virus infection. J Virol 2007;81:5036-5045.

3. Kato T, Choi Y, Elmowalid G, Sapp RK, Barth H, Furusaka A, Mishiro S, Wakita T, Krawczynski K, Liang TJ. Hepatitis C virus JFH-1 strain infection in chimpanzees is associated with low pathogenicity and emergence of an adaptive mutation. Hepatology 2008;48:732-740.

4. Kato T, Date T, Miyamoto M, Sugiyama M, Tanaka Y, Orito E, Ohno T, Sugihara K, Hasegawa I, Fujiwara K, Ito K, Ozasa A, Mizokami M, Wakita T. Detection of anti-hepatitis C virus effects of interferon and ribavirin by a sensitive replicon system. J Clin Microbiol 2005;43:5679-5684.

5. van den Hoff MJ, Moorman AF, Lamers WH. Electroporation in 'intracellular' buffer increases cell survival. Nucleic Acids Res 1992;20:2902.

6. Kato T, Date T, Murayama A, Morikawa K, Akazawa D, Wakita T. Cell culture and infection system for hepatitis C virus. Nat Protoc 2006;1:2334-2339.

7. Takeuchi T, Katsume A, Tanaka T, Abe A, Inoue K, Tsukiyama-Kohara K, Kawaguchi R, Tanaka S, Kohara M. Real-time detection system for quantification of hepatitis C virus genome. Gastroenterology 1999;116:636-642.

8. Aoyagi K, Ohue C, Iida K, Kimura T, Tanaka E, Kiyosawa K, Yagi S. Development of a simple and highly sensitive enzyme immunoassay for hepatitis C virus core antigen. J Clin Microbiol 1999;37:1802-1808.

9. Tateno C, Yoshizane Y, Saito N, Kataoka M, Utoh R, Yamasaki C, Tachibana A, Soeno Y, Asahina K, Hino H, Asahara T, Yokoi T, Furukawa T, Yoshizato K. Near completely humanized liver in mice shows human-type metabolic responses to drugs. Am J Pathol 2004;165:901-912.

10. Shiina M, Rehermann B. Cell culture-produced hepatitis C virus impairs plasmacytoid dendritic cell function. Hepatology 2008;47:385-395.

FIGURE LEGEND

Supporting Fig. 1.

Effects of mutations in non-structural regions on virus replication in HuH-7 cells

(A) Five μg RNA, synthesized by *in vitro* transcription of pSGR-JFH-1/Luc/wt, S1, S2, and C, were transfected into 1×10^6 cells by electroporation. The replication efficiency of these strains was determined by measuring firefly luciferase activities at indicated time-points, and expressed as fold increase of 4h levels. $*p < 0.00005$ compared to SGR-JFH-1/Luc/wt and S1. (B) Replication efficiency of pSGR-JFH-1/Luc/S2-NS3, S2-NS4B, S2-NS5A and S2-NS5B, determined as described in A. $*p < 0.005$ compared to SGR-JFH-1/Luc/wt.

Supporting Fig. 2.

Apoptosis induction in Huh-7.5.1 cells transfected with JFH-1/wt, S2 and their subgenomic replicons

Three million cells were transfected with 3 μg *in vitro* transcribed full-genome RNA of JFH-1/wt and S2 (A, B), or subgenomic replicon RNA of SGR-JFH1/Luc/wt and S2 (C). Apoptosis was detected by TUNEL assay without treatment (A) or after exposing cells to 100 ng/mL FasL plus 50 ng/mL Act D (B) or 20 ng/mL TNF-α plus 50 ng/mL Act D (C). The clone names and apoptosis induction indexes are indicated in the upper right box. Representative data of 3 independent experiments are shown.

Supporting Table 1.

Introduced non-synonymous mutations in the JFH-1 genome

		Name of Strains		
Region	Mutations	JFH-1/S1	JFH-1/S2	JFH-1/C
E2	N397S	+	+	
	K610R			+
P7	L752V		+	
NS2	G838R	+	+	+
	A878V		+	
	V881A	+	+	
NS3	T1077A		+	
NS4B	V1839A		+	
NS5A	A2075V			+
	Y2103C			+
	V2132A		+	
	Q2163R		+	
	S2223G			+
	P2271A		+	
	S2279N		+	
	F2281L		+	
	P2381L	+	+	
	A2389T	+	+	
	Q2412E	+	+	
NS5B	I2453V		+	
	A2640G		+	
	Q2883R			+
	S2915F			+

'+' indicates mutations observed

Supporting Table 2.

Infectious virus production and release of JFH-1 variants with mutations detected in JFH-1/S2 strain

Strain	Intracellular			Extracellular	Secretion Ratio (extra-/intra-)
	HCV RNA (copies/ μg RNA)	Infectivity Titer (ffu/well)	Specific Infectivity (ffu/copies)	Infectivity Titer (ffu/well)	
JFH-1/wt	4.38×10^{8} ± 1.43×10^{8}	1.60×10^{2} ± 2.67×10^{1}	2.21×10^{-7} ± 9.39×10^{-8}	7.81×10^{2} ± 5.74×10^{1}	4.9 ± 0.8
JFH-1/S2	2.91×10^{8} ± 6.11×10^{7}	$2.72 \times 10^{3*}$ ± 4.25×10^{1}	$3.72 \times 10^{-6*}$ ± 4.97×10^{-7}	$1.60 \times 10^{4*}$ ± 3.31×10^{3}	5.9 ± 1.3
JFH-1/ S2-wt	4.47×10^{8} ± 8.20×10^{6}	1.72×10^{3} ± 6.54×10^{2}	$2.00 \times 10^{-6*}$ ± 8.53×10^{-7}	$9.50 \times 10^{3*}$ ± 1.02×10^{3}	6.0 ± 2.1
JFH-1/ N397S	5.32×10^{8} ± 1.66×10^{8}	2.28×10^{2} ± 4.25×10^{1}	2.12×10^{-7} ± 3.72×10^{-8}	$1.09 \times 10^{3*}$ ± 3.86×10^{2}	4.8 ± 1.5
JFH-1/ L752V	5.52×10^{8} ± 1.60×10^{8}	$6.96 \times 10^{2*}$ ± 1.94×10^{2}	$8.90 \times 10^{-7*}$ ± 1.03×10^{-7}	$3.90 \times 10^{3*}$ ± 9.73×10^{2}	5.9 ± 2.2
JFH-1/ S2-NS2	5.14×10^{8} ± 5.02×10^{7}	1.09×10^{3} ± 5.54×10^{2}	1.20×10^{-6} ± 6.57×10^{-7}	$5.01 \times 10^{3*}$ ± 6.05×10^{2}	5.5 ± 2.8
JFH-1/ G838R	5.77×10^{8} ± 1.24×10^{8}	$7.82 \times 10^{2*}$ ± 1.53×10^{2}	$6.80\times 10^{-7*}$ ± 3.40×10^{-8}	$4.07 \times 10^{3*}$ ± 1.01×10^{3}	5.2 ± 1.0
JFH-1/ A878V	5.45×10^{8} ± 6.35×10^{7}	1.86×10^{2} ± 4.58×10^{1}	2.20×10^{-7} ± 6.09×10^{-8}	9.12×10^{2} ± 1.16×10^{2}	5.0 ± 0.7

*$p < 0.05$ compared with JFH-1/wt